



FEATURE ARTICLE

Modelling the effects of chromatic adaptation on phytoplankton community structure in the oligotrophic ocean

A. E. Hickman^{1,2,*}, S. Dutkiewicz², R. G. Williams¹, M. J. Follows²

¹Department of Ocean and Earth Sciences, University of Liverpool, Liverpool L69 3GP, UK

²Department of Earth, Atmospheric and Planetary Sciences, Massachusetts Institute of Technology, Cambridge, Massachusetts 01239, USA

ABSTRACT: We explored the role of chromatic adaptation in shaping vertical phytoplankton community structures using a trait-based ecosystem model. The model included 1000 'phytoplankton types' and was applied to the oligotrophic South Atlantic Gyre in a 1-dimensional framework, where 'phytoplankton types' refers to the model phytoplankton that were stochastically assigned unique physiological characteristics. The model incorporates multi-spectral optics and light absorption properties for the different phytoplankton. The model successfully reproduced observed vertical gradients in the nitrate, bulk phytoplankton properties and community structure. Model phytoplankton types with *Synechococcus*-like spectral light absorption properties were outcompeted at depth, where eukaryote-like spectral properties were advantageous. In contrast, photoinhibition was important for vertical separation of high-light and low-light *Prochlorococcus* model analogues. In addition, temperature dependence was important for selection of phytoplankton types on the temperature gradient. The fittest, or successful, phytoplankton types were characterised by combinations of simultaneously optimal traits that suited them to a particular depth in the water column, reflecting the view that phytoplankton have co-evolved multiple traits that are advantageous in a particular environmental condition or niche.

KEY WORDS: Phytoplankton · Chromatic adaptation · Photosynthesis · Niche · Modelling · Species · Selection · Pigments

Resale or republication not permitted without written consent of the publisher



The underwater light spectrum provides a complex environment for phytoplankton photosynthesis and growth.

Image: Alex Mustard (amustard.com)

INTRODUCTION

Phytoplankton community composition varies widely over the global ocean resulting from differences in fitness and species selection in the physical, chemical and predatory environment. Relative fitness of phytoplankton is determined by a number of factors, including the growth dependence on nutrient availability, light and temperature, as well as susceptibility to predation, viral lysis and other causes of mortality.

*Email: ahickman@liv.ac.uk

In the open ocean, oligotrophic environment of the extensive subtropical gyres, there is distinct vertical structuring of the habitats of the pico-phytoplankton (Fig. 1): *Synechococcus* usually occupy surface waters, whilst eukaryotes and *Prochlorococcus* occur throughout the water column, normally with subsurface biomass maxima (Partensky et al. 1996, Zubkov et al. 2000). Vertical gradients among different *Prochlorococcus* ecotypes have also been observed in oligotrophic regions (Moore et al. 1998, Johnson et al. 2006). In these stratified water columns, the vertical gradients in phytoplankton community structure are coincident with gradients in temperature, nutrient and light availability. Our aim was to explore how these environmental factors act in forming the observed phytoplankton distributions. We examined the hypothesis that, through their pigment compositions, the spectral light absorption characteristics of different phytoplankton are important in determining species selection in the spectral light gradient (Bidigare et al. 1990a, Moore et al. 1998, Sathyendranath & Platt 2007, Hickman et al. 2009).

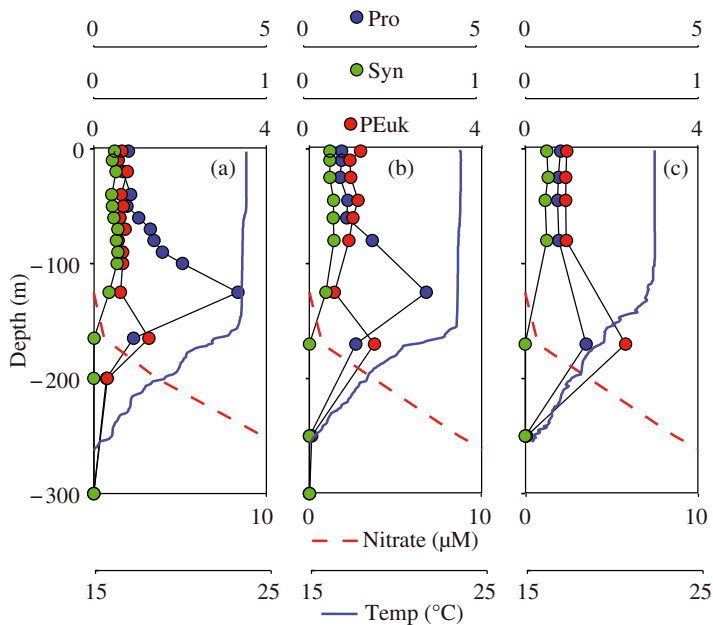


Fig. 1. (a to c) Vertical profiles of carbon biomass (mg C m^{-3}) of *Synechococcus* (Syn), *Prochlorococcus* (Pro) and picoeukaryotes (PEuk) along with corresponding temperature and nitrate profiles at (d) 3 locations in the South Atlantic Gyre. Data were obtained on (a) 14, (b) 15 and (c) 17 October 2004 (nitrate in Panel c from 15 October). Analytical flow cytometry measurements provided by J. Heywood and M. Zubkov

Our study complements the work of Stomp et al. (2004, 2007), who illustrated the importance of spectral light absorption properties on the coexistence of 2 species of *Synechococcus* in laboratory cultures and an idealised model. Previous modelling studies have also explored the importance of differences in photo-physiology for niche separation of *Synechococcus* and *Prochlorococcus* (Rabouille et al. 2007), and have incorporated spectral light absorption properties in global phytoplankton functional type models (e.g. Gregg & Casey 2007). Here, we used an ecosystem model to explicitly explore the role of different traits, specifically the nutrient, temperature and spectral light dependencies, in the competition among and selection for different phytoplankton taxa, and thus in forming observed distributions.

We focussed our study on the South Atlantic Gyre, which is broadly representative of much of the oligotrophic ocean (Fig. 1). The physical environment is relatively stable and has relatively weak temporal variability. We used a trait-based modelling approach (Follows et al. 2007) that was modified to include multi-spectral optics and light absorption characteristics for different phytoplankton. In the model, traits were assigned stochastically for a large number of 'phytoplankton types', where each phytoplankton type has a unique combination of parameter values that govern its growth dependencies with respect to light, nutrients and temperature. In this framework, phytoplankton community structure is an emergent property resulting from the interaction, competition and selection of phytoplankton types in the virtual ocean environment. We explored the model outcomes and a series of model 'thought experiments' to investigate, in particular, the role of the spectral composition of *in situ* irradiance and phytoplankton light absorption, along with nutrient and temperature dependence on growth, in shaping the habitats of the fit and abundant phytoplankton types.

OBSERVATIONAL CONTEXT

To provide a context for the study, we first considered the phytoplankton distributions observed in the South Atlantic Gyre (Fig. 1). Data were collected on the Atlantic Meridional Transect (AMT-15 from the UK to Cape Town, South Africa, 17 September to 29 November 2004), including information on the vertical distributions of *Prochlorococcus*, *Synechococcus* and picoeukaryotes, where the latter represent a mixed group of small eukaryotes ($\sim 2 \mu\text{m}$). Abundances of these cells were measured by analytical flow cytometry following methods of Heywood et al. (2006) and using the constant biomass conversion factors of

Zubkov et al. (1998). These small cells accounted for ~80% of the phytoplankton chlorophyll *a* (chl *a*), as measured by size fractionation. *Synechococcus* were restricted to the surface mixed layer (Fig. 1), whilst *Prochlorococcus* and picoeukaryotes together dominated the biomass throughout the water column. Both *Prochlorococcus* and picoeukaryotes exhibited subsurface biomass peaks. The vertical gradients in the phytoplankton community structure are broadly persistent over the South Atlantic Gyre (Fig. 1), and are in accord with previous observations in the region (Zubkov et al. 2000), and those in other oligotrophic regions (Partensky et al. 1996). Vertical gradients in different *Prochlorococcus* ecotypes have also been observed in the South Atlantic Gyre (Johnson et al. 2006).

A variety of differences between *Synechococcus*, eukaryotes and *Prochlorococcus* ecotypes may contribute to their interactions and species selection, including their distinct pigment compositions. Specifically, and in addition to other pigments, *Synechococcus* contain phycobiliproteins that absorb light between 495 and 620 nm, whilst eukaryotes contain various photosynthetic carotenoids that absorb light of 490 to 510 nm (Bidigare et al. 1990b, Jeffrey et al. 1997; Fig. 2). Only a minority of eukaryotes also contain phycobiliproteins (Jeffrey et al. 1997). Similarly, *Prochlorococcus* has high-light and low-light ecotypes that differ in their pigment ratios (particularly divinyl chl *b*:divinyl chl *a*), leading to preferential absorption of light at different wavelengths (Moore et al. 1995; Fig. 2).

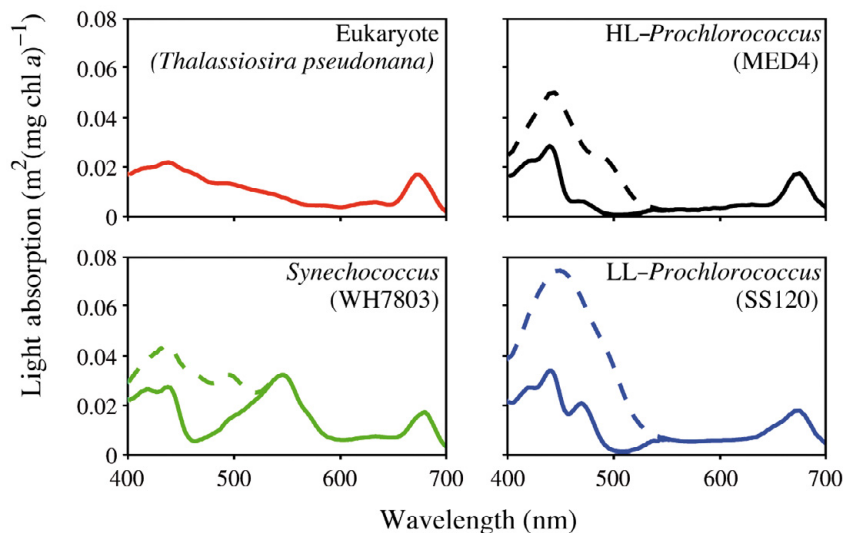


Fig. 2. Chlorophyll (chl) *a*-normalised light absorption spectra for 4 different phytoplankton types. HL: high-light; LL: low-light. Measurements were made on cultured phytoplankton under similar growth irradiances. Solid lines show light absorbed only by photosynthetic pigments ($a_{ps}^{chl}(\lambda)$); dashed lines show the light absorbed by all pigments ($a^{chl}(\lambda)$). Difference between the solid and dashed lines subsequently illustrates the amount and spectral distribution of light absorbed by the non-photosynthetic carotenoids. There was a negligible amount of such pigments in the eukaryotes. Culture data provided by L. Moore and D. Suggett

Vertical gradients in the phytoplankton community structure are reflected in pigment concentrations and lead to shifts in relative light absorption with depth (Babin et al. 1996, Barlow et al. 2002). For the South Atlantic Gyre, the ratio of phytoplankton light absorption at 490:550 nm increased from 0.62 at the surface to 0.73 at depth, reflecting a shift in phytoplankton light harvesting from the green to blue part of the light spectrum. Light absorption measurements during AMT-15 were made following Hickman et al. (2009) based on the methods of Bricaud & Stramski (1990).

MODEL

The multi-species model was based on that of Follows et al. (2007) and was applied in a 1-dimensional framework for a location in the South Atlantic Gyre (17.5° S, 24.5° W). The model was significantly modified so that light dependence of growth for the different phytoplankton types was determined from assigned light absorption spectra from culture data, and a parameterisation of photophysiology was introduced, based on Geider et al. (1997). In the following sections, we briefly describe relevant aspects of the model and the modifications.

Physics and biogeochemistry. The foundation of the stochastic phytoplankton-modelling framework, and the parameterisations therein, were described by Follows et al. (2007) with modifications as in Dutkiewicz et al. (2009). Here the model was configured to resolve only the vertical dimension, with a resolution of 10 m from the surface to a depth of 150 m, 20 m for the next 100 m, and gradually increasing thickness with depth thereafter. Mixed layer deepening and shoaling were achieved by a simple convective adjustment parameterisation driven by a relaxation of sea surface temperature towards the climatological seasonal cycle on a timescale of 3 d (World Ocean Atlas; Stephens et al. 2002). A background diapycnal diffusivity of $10^{-5} \text{ m}^2 \text{ s}^{-1}$ was also imposed, in accord with observations from the subtropical thermocline (Ledwell et al. 1993).

As in Dutkiewicz et al. (2009), the model includes the cycling of nitrogen and phosphorus (as well as iron and silicate) and a relatively simple parameterisation of the remineralisation of organic matter by heterotrophic microbes and assumes fixed Redfieldian elemental ratios in phytoplankton

(120:16:1 C:N:P). Given the focus of the current study, no large phytoplankton types were initialised, no types required silicate, and iron concentrations were maintained so that iron was never limiting.

A climatological annual cycle of 24 h mean irradiance for the South Atlantic Gyre location, obtained from Sea-viewing Wide Field-of-view Sensor (SeaWiFS) photosynthetically available radiation (PAR) data, was imposed at the surface. Initial nutrient fields were obtained from the World Ocean Atlas 2001 (Conkright et al. 2002), and the delivery of nitrate and phosphate due to lateral advection and isopycnal transfer, important in oligotrophic gyres (Williams & Follows 1998, Dutkiewicz et al. 2005), was parameterised by additional sources throughout the upper 200 m. The imposed convergence of lateral fluxes ($0.00125 \mu\text{M P yr}^{-1}$ and $0.02 \mu\text{M N yr}^{-1}$) were consistent with those inferred from climatological data (Williams & Follows 1998) and as diagnosed in a 3-dimensional model (Dutkiewicz et al. 2009).

Spectral irradiance. The ecosystem model here differed from the previously published configurations (Follows et al. 2007, Dutkiewicz et al. 2009) in terms of the treatment of light and photophysiology. Here we resolved the wavelength composition by considering irradiance at 13 wavelengths between 400 and 700 nm, more than the minimum of 6 recommended by Kettle & Merchant (2008). The (normalised) wavelength spectrum of incident irradiance was obtained from optics profile data collected in the South Atlantic Gyre region during AMT-15 (via extrapolation of the light intensity at available wavelengths to the surface), and was scaled by the incident PAR to spectrally resolve incident irradiance. The seasonal change in the incident light spectrum was not considered, but is minimal compared to the variation with depth.

Penetration of irradiance, I ($\mu\text{mol photons m}^{-2} \text{s}^{-1}$) for each of the 13 wavelengths, λ (nm), was obtained at each depth, z_k (m),

$$I(\lambda, z_{k+1/2}) = I(\lambda, z_{k-1/2}) \exp[-k_d(\lambda, z_k)(z_{k+1/2} - z_{k-1/2})] \quad (1)$$

where $z_{k-1/2}$ and $z_{k+1/2}$ refer to the depths of the top and bottom of the depth bin respectively, and subscript k is a counter for the depth bin. The spectral light attenuation, $k_d(\lambda, z_k)$ (m^{-1}), was calculated from the attenuation by water, $k_{d,w}(\lambda)$ (Pope & Fry 1997), colored dissolved organic matter (CDOM), $k_{d,cdom}(\lambda)$ (from Kitidis et al. 2006 using coefficients from the South Atlantic Gyre region) and phytoplankton,

$$k_d(\lambda, z_k) = k_{d,w}(\lambda) + k_{d,cdom}(\lambda) + \sum_j [a_j^{\text{chl}}(\lambda) \text{chl}_j(z_k)] \quad (2)$$

where the attenuation by phytoplankton was summed over all phytoplankton types, j . $a_j^{\text{chl}}(\lambda)$ is the chl a -normalised light absorption ($\text{m}^2 \text{mg}^{-1}$ chl a) for each

phytoplankton type at each of the 13 wavelengths, and $\text{chl}_j(z_k)$ is the chl a concentration ($\text{mg chl } a \text{ m}^{-3}$) for each phytoplankton type for the depth bin z_k . The irradiance used for calculating phytoplankton growth was the mean irradiance within the depth bin:

$$I(\lambda, z_k) = \exp(0.5\{\ln[I(\lambda, z_{k+1/2})] + \ln[I(\lambda, z_{k-1/2})]\}) \quad (3)$$

Total PAR was obtained from the sum of irradiance between 400 and 700 nm, assuming a linear interpolation between the 13 wavelengths.

Phytoplankton light absorption. Phytoplankton light absorption spectra were obtained from cultures of 4 species grown at similar growth irradiances, which were considered to be representatives of high-light *Prochlorococcus* (HLPro), low-light *Prochlorococcus* (LLPro), *Synechococcus* (Syn) and eukaryotes (Euk). The cultures were: *Prochlorococcus* MED4 and SS120 grown at $70 \mu\text{mol photons m}^{-2} \text{s}^{-1}$ (Moore & Chisholm 1999), *Synechococcus* WH7803 grown at $50 \mu\text{mol photons m}^{-2} \text{s}^{-1}$ (Suggett et al. 2004) and *Thalassiosira pseudonana* grown at $25 \mu\text{mol photons m}^{-2} \text{s}^{-1}$ (Suggett et al. 2009), respectively.

The light absorption by all pigments provided by the culture measurements ($a_j^{\text{chl}}(\lambda)$) was used in the calculation of light attenuation, whereas estimation of phytoplankton growth was based on light absorption only by photosynthetically active pigments ($a_{\text{ps},j}^{\text{chl}}(\lambda)$), thus ignoring absorption by non-photosynthetic carotenoids (Fig. 2). The light absorption spectrum for only the photosynthetic pigments ($a_{\text{ps},j}^{\text{chl}}(\lambda)$) was obtained by adjusting the measured light absorption spectra ($a_j^{\text{chl}}(\lambda)$) by the ratio of light absorption by non-photosynthetic to total pigments at each wavelength (Babin et al. 1996, Hickman et al. 2009). The wavelength-dependent ratio was obtained from pigment-reconstructed spectra, following the traditional pigment-reconstruction technique (Bidigare et al. 1990b, Hickman et al. 2009).

The relative pigment concentrations for the reconstructions were calculated by scaling the weight-specific absorption spectra for the main pigment groups (photosynthetic carotenoids, non-photosynthetic carotenoids, chl a , b and c and phycoerythrobilin-rich phycobilins relevant for the representative *Synechococcus*; Bidigare et al. 1990b) expected for each phytoplankton type (according to Jeffrey et al. 1997) in order to yield the lowest sum of residuals between the pigment-reconstructed and measured light absorption spectra. For each of the 4 phytoplankton types, the average residuals across all wavelengths was $< 0.0035 \text{ m}^2 \text{mg}^{-1}$ chl a . Weight-specific absorption coefficients for the divinyl chlorophylls present in *Prochlorococcus* were assumed to be the same as those of the monovinyl chlorophylls.

Phytoplankton growth. The growth rate, $P_j^C(\text{s}^{-1})$, of each phytoplankton type, j , was determined by the steady state solution of the light-growth dependency of

Geider et al. (1997), which provided a variable chl *a* concentration, and was thus a modification of Follows et al. (2007). The light-growth dependency was based on an exponential form of the carbon-specific photosynthesis versus irradiance curve, modified to resolve the visible spectrum,

$$P_j^C = P_{m,j}^C \left[1 - \exp\left(\frac{-\Lambda_j^I \theta_j}{P_{m,j}^C}\right) \right] \quad (4)$$

where P_j^C is the carbon specific growth rate, and $P_{m,j}^C$ (s^{-1}) is the maximum (light saturated) photosynthetic rate, given by

$$P_{m,j}^C = \mu_j \gamma_j^N \gamma_j^T \quad (5)$$

where μ_j is the maximum possible growth rate (s^{-1}), and γ_j^N and γ_j^T , reflect the degree of limitation by nutrients and temperature and have values between 0 and 1 (described below). The linear slope of the photosynthesis versus irradiance curve depends on the chl *a* to carbon ratio, θ_j (g:g), which varies with photoacclimation (Geider et al. 1997):

$$\theta_j = \frac{\theta_m}{1 + \frac{\Lambda_j^I \theta_m}{2P_{m,j}^C}} \quad (6)$$

Λ_j^I in Eqs. (4) and (6) is the instantaneous photosynthetic rate given the amount of light absorbed by the phytoplankton, which is determined from the spectral irradiance and spectral light absorption coefficient for each phytoplankton type,

$$\Lambda_j^I = \phi_m \sum_{\lambda=400}^{\lambda=700} a_{ps,j}^{\text{chl}}(\lambda) I(\lambda) \quad (7)$$

where ϕ_m is the maximum quantum yield of carbon fixation ($\text{mol carbon mol}^{-1}$ photons), and θ_m is the maximum possible value of the chl *a* to carbon ratio. Both parameters were assumed to be the same for all phytoplankton types ($\phi_m = 0.04$ mol carbon mol^{-1} photons and $\theta_m = 1/60$ g:g, typical values observed for phytoplankton; Kyewalyanga et al. 1998, Geider et al. 1997). Phytoplankton types were assumed to be fully acclimated to *in situ* irradiance, as in the steady state solution of Geider et al. (1997), which is reasonable given the daily mean irradiance used and the relatively stable nature of the oligotrophic environment. In addition, for the *Prochlorococcus*-like phytoplankton types, divinyl-chl *a* was assumed to be equivalent to chl *a* for all calculations.

For phytoplankton types assigned to be susceptible to photoinhibition, P_j^C was reduced depending on the ratio of irradiance, I (the total between 400 and 700 nm) to Ek_j ($\mu\text{mol photons m}^{-2} \text{s}^{-1}$) according to

$$P_{j,\text{inhib}}^C = P_j^C \kappa \frac{Ek_j}{\sum_{\lambda=400}^{\lambda=700} I(\lambda)} \quad (8)$$

Ek_j is the light saturation parameter and represents the intercept of the maximum ($P_{m,j}^C$) and the linear initial slope [$\theta_j \phi_m \overline{a_{ps,j}^{\text{chl}}}(\lambda)$] of the carbon-specific photosynthesis versus irradiance curve,

$$Ek_j = \frac{P_{m,j}^C}{\theta_j \phi_m \overline{a_{ps,j}^{\text{chl}}}(\lambda)} \quad (9)$$

where $\overline{a_{ps,j}^{\text{chl}}}(\lambda)$ is the mean light absorption by photosynthetically active pigments across wavelengths of 400 to 700 nm. Photoinhibition only acts when irradiance is greater than Ek_j . The degree of photoinhibition was set by a factor κ , here equal to 1.2; for simplicity, there is no spectral dependence included for photoinhibition.

The light-growth response for different phytoplankton types was thus based on the assigned light absorption properties ($a_{ps,j}^{\text{chl}}$), along with an associated susceptibility (or not) to photoinhibition.

The temperature-growth function was based on an Eppley curve (Eppley 1972), with each phytoplankton type assigned an envelope within which it grows efficiently (Follows et al. 2007):

$$\gamma_j^T = \frac{1}{\tau_1} \left(A^T \exp^{-B(T-T_{0,j})^C} - \tau_2 \right) \quad (10)$$

The coefficients defining the temperature envelope were the same for each phytoplankton type ($A = 1.04$, $B = 0.001$, $C = 4$, $\tau_1 = 3$ and $\tau_2 = 0.3$, all dimensionless, as in Dutkiewicz et al. 2009), except $T_{0,j}$ ($^{\circ}\text{C}$), the optimum temperature for growth, hereafter referred to as T_{opt} .

The nutrient-growth dependency γ_j^N was determined by the most limiting nutrient (Follows et al. 2007), with the individual nutrient limitations based on a Michaelis-Menten function, $N_i/(N_i + K_{ij})$, and modified for nitrogen to include inhibition of nitrate uptake by ammonium (Dutkiewicz et al. 2009); subscript i indicates the nutrient (phosphate, nitrate), N_i is the nutrient concentration (μM) and K_{ij} is the nutrient half-saturation constant (μM). Nutrient-growth dependencies differed between phytoplankton types according to the required sources of nitrogen and the half-saturation constant, K_{ij} , hereafter referred to as K_{sat} , which were translated for N and P according to the fixed Redfield stoichiometry.

The model included 2 grazers (as in Dutkiewicz et al. 2009), but since there were no imposed size differences between phytoplankton types in the current study, grazing did not influence the phytoplankton community structure.

Trait choices. Trait choices for the model phytoplankton types were assigned based on a series of coin flips and random selection of parameter values (Fig. 3). Phytoplankton types were assigned to 1 of 3 nutrient resource groups: a requirement for NH_4 only, NH_4 and

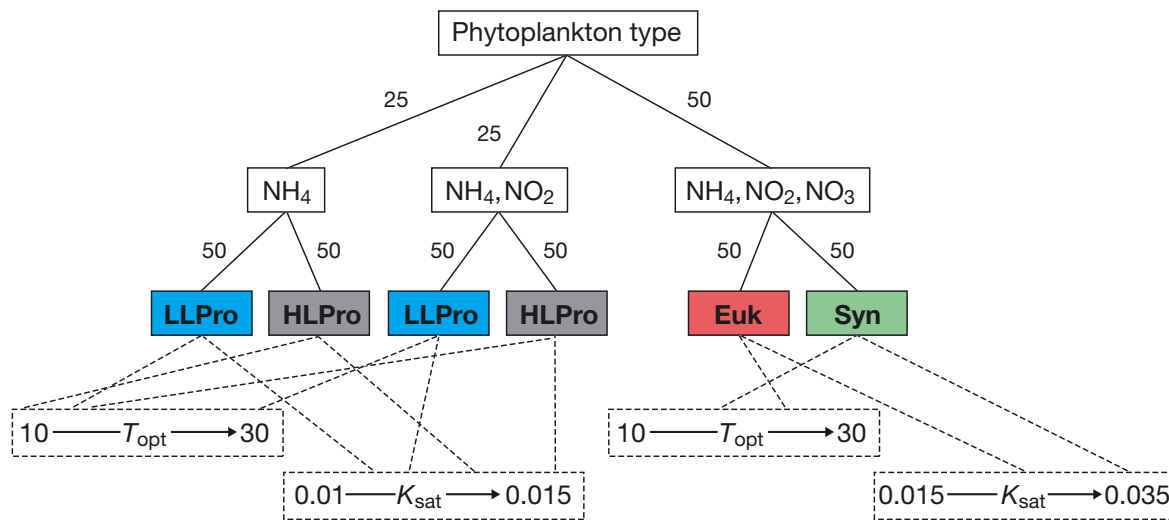


Fig. 3. Framework of choices and parameter ranges for growth characteristics during initialisation of the phytoplankton types. Each phytoplankton type was first assigned nitrogen resources and then allocated 1 of the 4 spectral light absorption properties (high-light *Prochlorococcus* [HLPro], low-light *Prochlorococcus* [LLPro], *Synechococcus* [Syn] or eukaryote [Euk], as in Fig. 2), depending on the requirement for nitrate. Then each phytoplankton type was stochastically assigned a value for temperature optima T_{opt} (°C) and half-saturation constant for nutrients, K_{sat} ($\mu\text{M P}$) within the given ranges (again ranges for K_{sat} depend on the nitrogen resource). Values for K_{sat} are translated between phosphorus and nitrogen using a fixed molar ratio (16:1 N:P). Numbers next to tree branches indicate the probability (%) of each choice. Photoinhibition was imposed on all phytoplankton types assigned light absorption properties of LLPro

NO_2 in combination, or NH_4 , NO_2 and NO_3 in combination, broadly reflecting possible combinations for phytoplankton (Moore et al. 2002). Within each nutrient resource group, phytoplankton types were assigned chl *a*-specific light absorption spectra according to Figs. 2 & 3. Superimposed onto this framework was a random selection for values for temperature optimum (T_{opt} ; Eq. 10) and half-saturation coefficient (K_{sat}) from plausible ranges (Fig. 3). The probability of trait choices was chosen so that a roughly equal number of phytoplankton types were assigned with each of the 4 different sets of light absorption properties (Fig. 3).

The phytoplankton types that did not require nitrate were assumed to be representative of *Prochlorococcus* and, thus, the lower K_{sat} range was a reasonable assumption given their small size (Chisholm 1992). Photoinhibition was imposed on phytoplankton types that were assigned LLPro absorption characteristics as suggested by culture studies (Moore et al. 1998, Six et al. 2007).

Model application and assessment. The model was initialised with 1000 phytoplankton types, which ensured that the possible trait parameter space was sufficiently well sampled to eliminate any significant dependence of the solutions on the stochastic initialisation. The model was integrated for 20 yr, after which time the annual cycles of nutrient fields and phytoplankton community structure were repeatable and consistent. All phytoplankton types were retained

throughout the model runs, even if their biomass was very low. Twenty different independent integrations ('ensemble members') were conducted, each with a unique stochastic initialisation of phytoplankton types. While each ensemble member resulted in a slightly different emergent community structure (a selection is shown in Fig. 4), importantly, the broad character of the vertical biogeography in each ensemble member was similar, and the ensemble mean was robust. The ensemble mean was obtained from the mean biomass of phytoplankton types when grouped according to light absorption properties and whether they use nitrate or not (Fig. 3). The notation e_{syn} , e_{euk} , e_{HLPro} , e_{LLPro} is used to refer to all phytoplankton types with Syn, Euk, HLPro and LLPro absorption properties, respectively, such that e_{syn} and e_{euk} use nitrate, while e_{HLPro} and e_{LLPro} do not.

We first assessed the skill of the model by comparing the ensemble mean to observations collected during AMT-15. Then we assessed the traits important to forming the community structure. This assessment was done by considering model outcomes as well as using the model to conduct a series of 'thought experiments'. Appendix 1 contains a suite of thought experiments that sequentially illustrate the roles of the light, nutrient and temperature dependencies in turn on the community structure. All model outcomes shown are for Month 10, in order to compare to AMT-15 data.

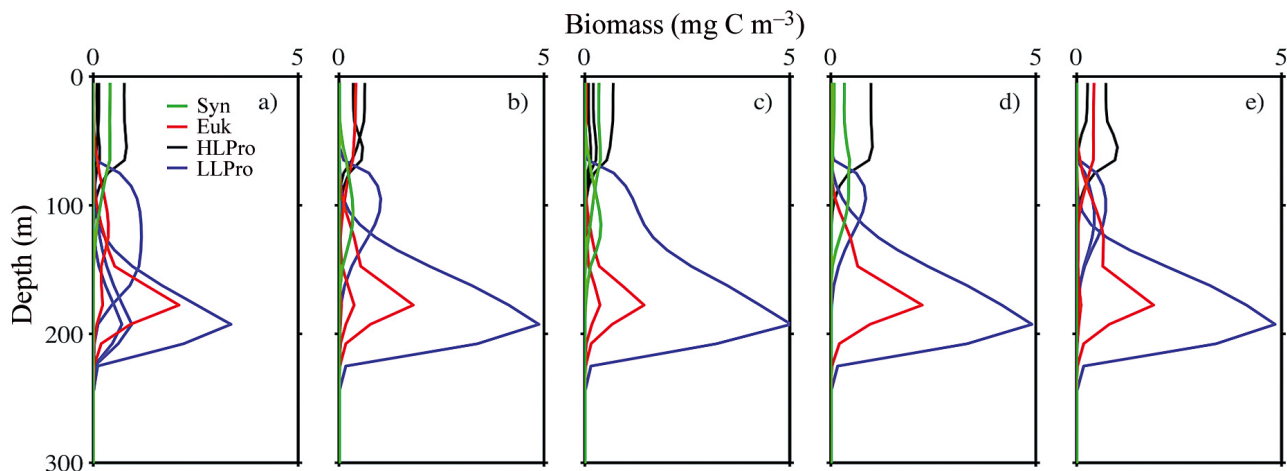


Fig. 4. Vertical profiles of carbon biomass for all 1000 phytoplankton types for 5 of the 20 ensemble members. Individual phytoplankton types are identified by colour according to their light absorption properties (Syn: *Synechococcus*; Euk: eukaryote; HLPro: high-light *Prochlorococcus*; LLPro: low-light *Prochlorococcus*). Multiple lines of the same colour therefore represent phytoplankton types with the same light absorption properties, but different values for the half-saturation constant (K_{sat}) and the optimum temperature for growth (T_{opt})

RESULTS

Nitrate, biomass and chlorophyll

We first compared the detailed hydrographic and biological gradients measured at one of the stations in the South Atlantic Gyre during AMT-15 (corresponding to Fig. 1c) to the mean ensemble outcome (Fig. 5). The model represented a shallower mixed layer than indicated in the (pre-dawn) observations (Fig. 5a,b), due to the monthly mean model output. Simulated nutrient, biomass and chl *a* profiles were consistent with the observations (Fig. 5a,b). The model successfully reproduced a deep chlorophyll maximum (DCM) coincident with the depth of the nitracline. The modelled absolute chl *a* concentrations were lower than observed, but the total carbon biomass for the phytoplankton was about the same as in the data at the surface as well as at the DCM, perhaps reflecting the assumption of instantaneous acclimation of chlorophyll to carbon ratios.

Phytoplankton community structure

The model qualitatively captured the observed gradients in community composition. The coexistence of phytoplankton types that use nitrate (assumed to represent eukaryotes and *Synechococcus*) and those that do not (assumed to represent *Prochlorococcus*) was reproduced in the model. Within the subset of nitrate-using phytoplankton types, the biomass maximum for those with Syn absorption spectra, e_{syn} , was shallower

in the water column than those with Euk absorption spectra, e_{euk} , consistent with the distributions of *Synechococcus* and picoeukaryotes in the data (Fig. 5c,d). Similarly, for the non-nitrate using types, the biomass maxima for those with HLPro absorption spectra, e_{HLPro} , was shallower than for those with LLPro absorption spectra, e_{LLPro} .

While the vertical structuring of niches seemed reasonable, the relative biomass of the different phytoplankton types differed, sometimes significantly, from that in the observations. For instance, the biomass of e_{syn} was overestimated and e_{euk} was underestimated at the surface (such that the biomass for e_{syn} was greater than e_{euk}), although at the DCM the biomass for each type was reasonable. Conversely, the combined biomass of e_{LLPro} and e_{HLPro} in the model was similar to the biomass of *Prochlorococcus* at the surface, but overestimated at the DCM. However, the important features reproduced by the model are: the surface bias of phytoplankton types with Syn absorption spectra, and their absence at depth; the ubiquity of phytoplankton types with Euk absorption spectra, and their biomass maximum at depth; the vertical separation of phytoplankton types with HLPro and LLPro absorption spectra; and the coexistence of the nitrate and non-nitrate using phytoplankton types. A traditional, after the fact ‘tuning’ of model parameters could in theory improve the quantitative comparisons, but this is not the philosophy of this self-assembling community approach. We therefore proceed by considering these qualitatively realistic and robust features of the vertical distributions.

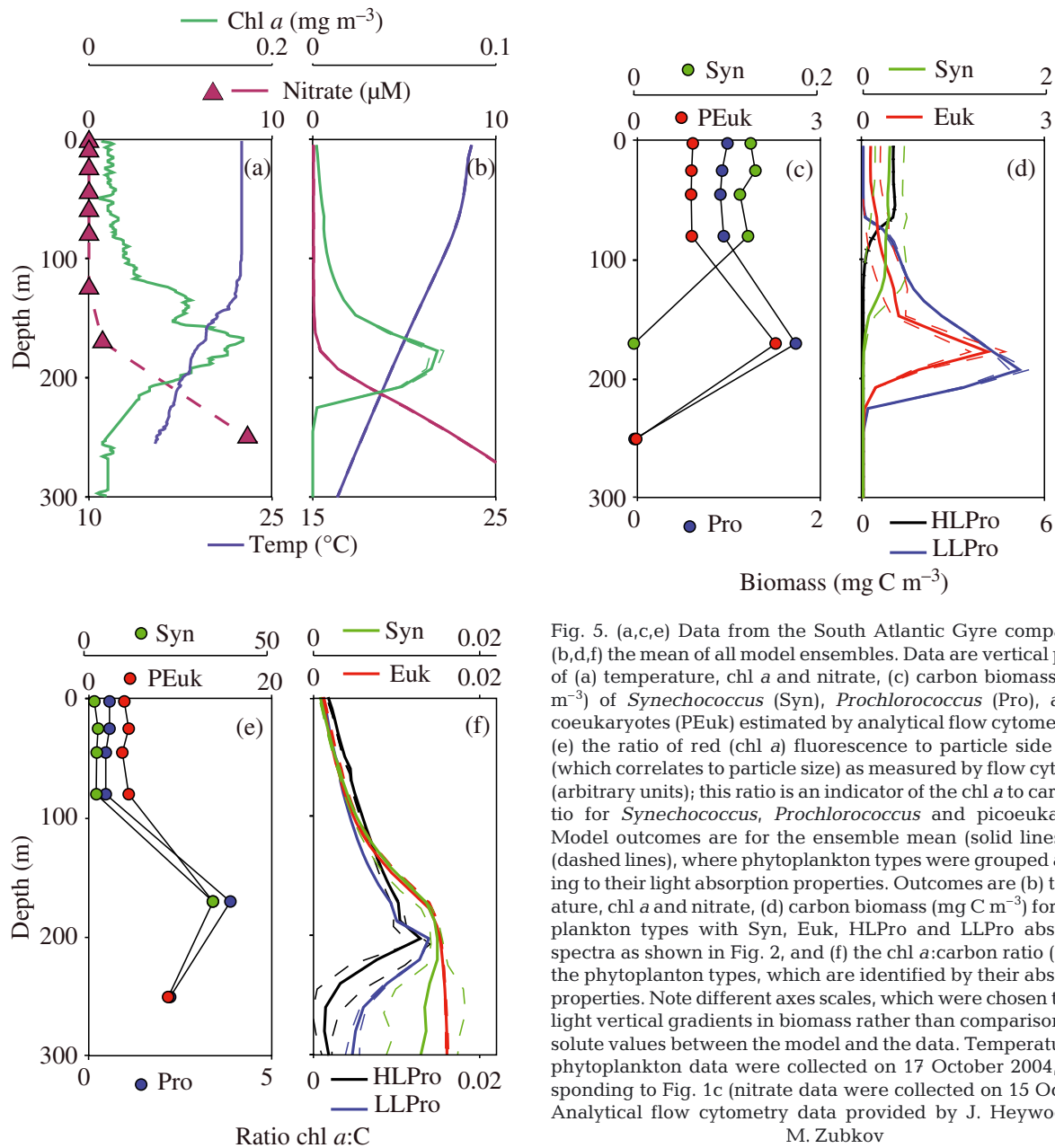


Fig. 5. (a,c,e) Data from the South Atlantic Gyre compared to (b,d,f) the mean of all model ensembles. Data are vertical profiles of (a) temperature, chl *a* and nitrate, (c) carbon biomass (mg C m⁻³) of *Synechococcus* (Syn), *Prochlorococcus* (Pro), and picoeukaryotes (PEuk) estimated by analytical flow cytometry and (e) the ratio of red (chl *a*) fluorescence to particle side scatter (which correlates to particle size) as measured by flow cytometry (arbitrary units); this ratio is an indicator of the chl *a* to carbon ratio for *Synechococcus*, *Prochlorococcus* and picoeukaryotes. Model outcomes are for the ensemble mean (solid lines) \pm SD (dashed lines), where phytoplankton types were grouped according to their light absorption properties. Outcomes are (b) temperature, chl *a* and nitrate, (d) carbon biomass (mg C m⁻³) for phytoplankton types with Syn, Euk, HLPro and LLPro absorption spectra as shown in Fig. 2, and (f) the chl *a*:carbon ratio (g:g) for the phytoplankton types, which are identified by their absorption properties. Note different axes scales, which were chosen to highlight vertical gradients in biomass rather than comparison of absolute values between the model and the data. Temperature and phytoplankton data were collected on 17 October 2004, corresponding to Fig. 1c (nitrate data were collected on 15 October). Analytical flow cytometry data provided by J. Heywood and M. Zubkov

Photophysiology of phytoplankton types

The ratio of phytoplankton chl *a* to carbon increased with depth in the model as a result of photoacclimation (Geider et al. 1997), as observed in the data (Fig. 5e,f). The available light spectrum became depleted in irradiance at 550 nm relative to 490 nm with depth, as observed in the data (Fig. 6a,d). Light was attenuated principally by water and, to a lesser extent by CDOM, which attenuate at the red and blue end of the light spectrum, respectively (Kirk 1994, Pope & Fry 1997, Kitidis et al. 2006). Attenuation by phytoplankton also modified the available light spectrum, but was a rela-

tively minor component of the light attenuation in this oligotrophic ocean.

The normalised light absorption spectra for the entire phytoplankton community at 2 depths in the model compared well to observations made during AMT-15 (Fig. 6b,e). Most importantly, the change in bulk community phytoplankton absorption spectra with depth was associated with changes in the wavelengths of available light through the water column. The shift in relative light absorption, notably from ~510–575 to 450–500 nm, between the surface and deep phytoplankton populations reflects utilisation of the available light field and results from contrasts in

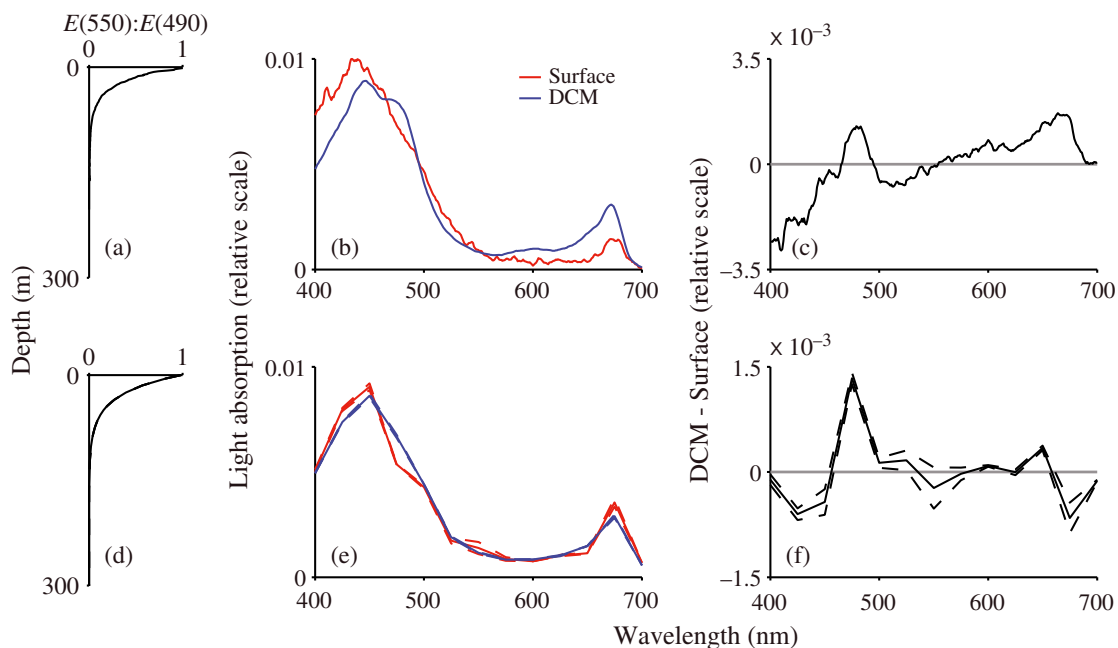


Fig. 6. (a,b,c) Data compared to (d,e,f) model outcomes. (a,d) ratio of irradiance E at 550 to 490 nm through the water column; (b,e) light absorption by the entire phytoplankton community near the surface (data = 20 m, model = 25 m) and the depth of the deep chl a maximum (DCM; data = 170 m, model = 177.5 m) normalised by the area of the spectra in each case; (c,f) difference in the (normalised) phytoplankton light absorption spectra at the DCM compared to at the surface. Positive values in (d) and (f) indicate an increase in relative light absorption at the DCM compared to the surface, whereas negative values indicate a decrease; the area under the curve is equal to 0 such that the y -axis is a relative scale. Data collected during AMT-15 on 17 October 2004, corresponding to Figs. 1c & 5 (optics data provided by G. Moore and L. Hay). Model outcomes are for the ensemble mean (solid lines) \pm SD (dashed lines)

community structure (Fig. 6c,f). This response in the model was not pre-assigned, but depends on the emergent phytoplankton community and their combined light absorption characteristics. Shifts in the wavelengths of phytoplankton light absorption in response to the available irradiance are indicative of chromatic adaptation and selection for phytoplankton in the spectral light gradient (Bidigare et al. 1990a, Lutz et al. 2003, Hickman et al. 2009).

Variance between ensemble members in the difference in relative light absorption between the surface and deep populations at 525 to 575 nm in the model (Fig. 6f) reflects whether types with Euk or Syn spectra dominated towards the surface (Fig. 4), although on average, the presence of types with Syn spectra towards the surface led to a decrease in relative light absorption at 550 nm with depth in the ensemble mean (Fig. 6f). Other contrasts in the deep and shallow spec-

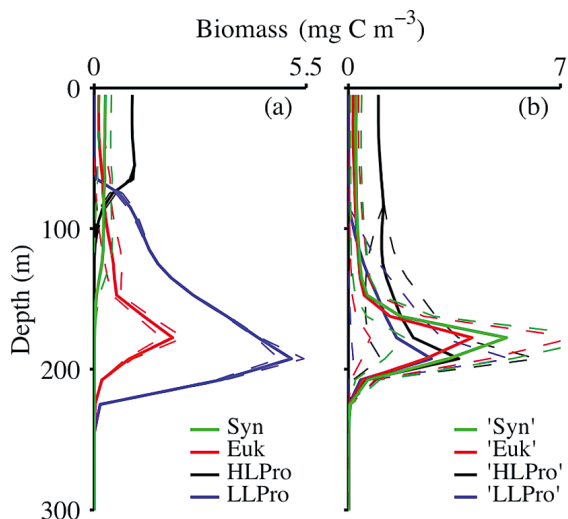


Fig. 7. Vertical profiles of carbon biomass for the ensemble mean (solid lines) \pm SD (dashed lines) where phytoplankton types are grouped based on their light absorption properties. (a) Outcome from the full model as in Fig. 5; (b) as in (a), but where all phytoplankton types were assigned the same spectral light absorption properties (specifically, all types were assigned light absorption spectra obtained from the mean, at each wavelength, of the HLPro, LLPro, Euk and Syn spectra shown in Fig. 2. Mean spectra were obtained for both the light absorption by all pigments, and the light absorption by photosynthetic pigments). Subsequently, as indicated by quotation marks, coloured lines in (b) represent the absorption spectra that would have been assigned for each phytoplankton type in the full model run, and thus direct comparison of (a) and (b) illustrates the role of the different light absorption spectra in forming the vertical distributions

tra between the data and the model, notably at 525 and 675 nm (Fig. 6b,c,e,f), likely resulted from our simplified community composition, although it is unlikely that phytoplankton absorption at the red part of the light spectrum plays a strong role in chromatic adaptation due to the absence of red light in most of the water column.

Given the broad agreement between the modelled and observed phytoplankton distributions and photo-physiology, what insights can the model provide into the key factors driving the community structure? In particular, is spectral irradiance, and hence chromatic adaptation, important for the selection of phytoplankton types in the model?

Drivers of phytoplankton selection

To assess the importance of different traits in forming the community structures, we considered the consistencies and differences between outcomes of the ensemble members (Fig. 4), as well as the ensemble mean (Fig. 7a). A suite of thought experiments was conducted to illustrate the effect of each of the temperature, nutrient and spectral light dependencies on the distribution of phytoplankton types in turn. This suite of experiments is described fully in Appendix 1. In addition, to focus on the role of the spectral light absorption properties, we considered an additional idealised experiment whereby the same 20 ensemble members as in the full model were re-run, this time with all phytoplankton types assigned identical light absorption spectra (Fig. 7a,b). The absorption spectrum assigned to all phytoplankton types in this idealised experiment was the mean of the representative spectra in Fig. 2 (at each wavelength, and for spectra for both all-pigments and only photosynthetic pigments).

We start by considering the role of the spectral light dependence in determining the distribution of phytoplankton types that utilise nitrate and those that do not, and then explored the vertical gradients in community structure within these 2 broad groups.

Light absorption properties and utilisation of nitrate

Nitrate-using (e_{syn} and e_{euk}) and non-nitrate-using (e_{HLP} and e_{LLP}) phytoplankton types coexisted throughout the water column in all ensemble members of the full model (Figs. 4 & 5d). The relative biomasses of these 2 groups were consistent throughout much of the water column, although the ratio of non-nitrate- to nitrate-using types increased at the DCM. In the idealised experiment, where phytoplankton types were

assigned identical light absorption spectra (Fig. 7b), the nitrate- and non-nitrate-using types coexisted throughout most of the water column at a ratio consistent with that shown for the full model (Fig. 7a). However, at the DCM in the full model (Fig. 7a), the biomass for the phytoplankton types that used nitrate (e_{euk}) was less than for types that did not (e_{LLP}), whilst in the idealised experiment, the relative biomasses of these 2 groups were similar (Fig. 7b). Thus, the spectral absorption properties of LLPro appear to be advantageous at depth, compared to the absorption properties of Euk. It follows that the nutrient dependence was the dominant factor determining the coexistence between the nitrate- and non-nitrate-using phytoplankton types, but light absorption properties also contributed to the dominance of the e_{LLP} at the DCM. Specifically, the lower possible K_{sat} value assigned to the phytoplankton types that do not use nitrate (trading off the cost of reducing nitrate against general nutrient affinity) was the first-order factor determining the coexistence, whilst LLPro absorption properties provided a second-order advantage in the deeper, bluer, part of the water column.

Role of light absorption properties for phytoplankton that do not use nitrate

The non-nitrate-using phytoplankton types differed according to their light absorption properties (and photoinhibition) as well as their ability to utilise NO_2 along with NH_4 , or to use NH_4 only (Fig. 3).

Sensitivity tests showed that without photoinhibition, phytoplankton types with LLPro absorption spectra out-competed those with HLP spectra at all depths. Thus, spectral light absorption properties alone were not sufficient to separate e_{LLP} and e_{HLP} in the light gradient. Including photoinhibition for all phytoplankton types with LLPro absorption properties, representing a trade-off for their efficient light harvesting, obtained realistic vertical distributions of e_{LLP} and e_{HLP} (Fig. 5d).

When implemented in the model, photoinhibition had a dominant affect on the vertical gradients of the phytoplankton types that did not use nitrate, causing dominance of e_{HLP} and exclusion of e_{LLP} towards the surface (Figs. 4 & 5e). At depth, the competitive exclusion of e_{HLP} by e_{LLP} occurred due to the advantageous light absorption properties of LLPro (Figs. 4 & 5e), as confirmed by comparison to the idealised experiment where there was no competition for spectral irradiance (Fig. 7a,b). The dominance of e_{HLP} near the surface and e_{LLP} at depth occurred in all ensemble members of the full model, such that these features of the community structure were robust even given any combination of initialised T_{opt} and K_{sat} values (Figs. 4 & 5e).

Laboratory and field observations suggest that photoinhibition is important for the general absence of some low-light *Prochlorococcus* ecotypes in surface waters (Moore & Chisholm 1999, Zinser et al. 2007), although there are likely to be other or additional trade-offs important to the niche separation of these organisms (Zinser et al. 2007). Culture studies have shown that a low-light *Prochlorococcus* ecotype (SS120) is more susceptible to photoinhibition than a high-light strain due to a relatively slow repair rate of photo-damaged photosystem-II's (Six et al. 2007). All *Prochlorococcus* ecotypes may be more susceptible to photoinhibition than other phytoplankton due to the presence of divinyl chlorophylls, which are considered to be more expensive to repair than the monovinyl chlorophyll forms (Tomo et al. 2009). The low-light *Prochlorococcus*, with a high divinyl chl *b*:divinyl chl *a* ratio, are adapted to highly efficient utilisation of blue light at depth, while the relatively less efficient light absorption properties of high-light *Prochlorococcus*, with a low divinyl chl *b*:divinyl chl *a* ratio, presumably reflects a balance between light absorption for photosynthesis and minimising the risk of photodamage.

In the model, the utilisation of different nitrogen sources was also important for the vertical distributions of phytoplankton types that did not use nitrate, representing *Prochlorococcus*. At the DCM, and thus at the nutricline, e_{LLP} that used NO_2 as well as NH_4 had a competitive advantage compared to those that only used NH_4 . In contrast, near the surface where NO_2 concentrations were low, e_{HLP} that utilised NO_2 as well as NH_4 did not have a significant advantage. This preference for reduced nitrogen source is consistent with culture studies showing that low-light *Prochlorococcus* ecotypes assimilate NO_2 as well as NH_4 , whilst cultured high-light ecotypes have lost the ability to use NO_2 (Moore et al. 2002, Rocap et al. 2003). The model therefore supports the view that this trait is also important for niche partitioning of different *Prochlorococcus* ecotypes on vertical nutrient gradients (Moore et al. 2002, Bragg et al. 2010).

Role of light absorption properties for phytoplankton that use nitrate

The group of phytoplankton types that use nitrate consisted of phytoplankton with Syn and Euk spectral absorption properties.

In the idealised experiment without competition for spectral irradiance (Fig. 7b), the biomass of the phytoplankton types that had, in the full model, been assigned Syn and Euk absorption properties (the red and green lines in Fig. 7b) followed the same vertical gradient; their slight difference in absolute biomass

was due to the stochastic assignment of T_{opt} and K_{sat} for the phytoplankton types within each group, and this difference was not significant. It was therefore the light absorption properties that had resulted in the vertical gradients of these phytoplankton types in the full model (Figs. 5d & 7a). The phytoplankton types with Syn absorption spectra (e_{syn}) were not successful at the depth of the DCM in any ensemble member due to their competitive exclusion by those with Euk absorption spectra (e_{euk} ; Fig. 4), something that could not be overcome by any co-assigned combination of T_{opt} and K_{sat} values within the given ranges (Figs. 4 & 5e).

Towards the surface, however, the competition between e_{syn} and e_{euk} was more complicated. Whether a phytoplankton type with Syn or Euk absorption properties dominated near the surface varied between ensemble members (Fig. 4), and thus depended on the values of T_{opt} and K_{sat} for the corresponding phytoplankton types. Overall, however, types with Syn absorption properties had a competitive advantage over those with Euk spectra as evidenced by their higher biomass in the ensemble mean (Fig. 5). At 25 m in the ensemble mean, the biomass of e_{syn} was significantly greater than the biomass of e_{euk} at the 95 % confidence level (according to a *t*-test).

In an additional idealised experiment where all of their other traits were equal, phytoplankton types with absorption spectra of Syn and Euk coexisted towards the surface (see Appendix 1: Test 1, Fig. A1b for the full description of this experiment). This coexistence occurs due to their utilisation of different components of the light spectrum (Stomp et al. 2004, 2007), resulting in similar light-dependent growth rates. In the full model, the spectral absorption properties of these phytoplankton types thus play a less dominant role, allowing other traits to 'tip-the-balance' and be more significant in forming the resulting distributions.

The light absorption properties affect the growth rate according to Eq. (7). The value of the summed component, and therefore Λ_j^I , increases when the light absorption spectrum is similar to the wavelength composition of available light (Sathyendranath & Platt 2007). For the light field of the ensemble mean state, the value of Λ_j^I was 20 % higher for phytoplankton types with Syn compared to Euk absorption spectra at 25 m, but the growth rate (s^{-1}) was only 1 % greater (given the nutrient fields from the ensemble mean and assuming that all other characteristics were equal: $T_{\text{opt}} = 22^\circ\text{C}$ and $K_{\text{sat}} = 0.01$). This small difference in growth rate is partly due to compensation by photoacclimation, which results in a different chl *a* to carbon ratio between the phytoplankton types (0.025 and 0.030 g:g for the type with Syn and Euk absorption spectra, respectively). In contrast, the value of Λ_j^I and the growth rate were both 5 % higher for the phyto-

plankton types with Euk compared to Syn absorption spectra at 170 m, where the ratio of chl a to carbon was near maximal. Thus, the light absorption properties had a greater influence on growth rate at depth, and led to competitive exclusion of e_{syn} by e_{euk} in the full model, even for any combination of T_{opt} and K_{sat} values within the prescribed ranges (Figs. 3 & 4). The importance of the light absorption properties at depth reflects the fact that Λ_j^I determines the light-limited slope of the photosynthesis versus irradiance curve and hence light-limited growth rate (Eqs. 4 and 6). The absence of phytoplankton types with Syn absorption spectra at depth in the model is consistent with *Synechococcus* being light-limited due to their spectral light requirements (Wood 1985). Our model indicated that phytoplankton types with Syn absorption proper-

ties could survive at depth, were it not for their competitive exclusion by e_{euk} .

The slight advantage of phytoplankton types with Syn compared to Euk absorption properties towards the surface implies some light limitation of growth. The precise ratio of the biomass of these types (such as in Appendix 1: Test 1, Fig. A1b) is likely to result from a subtle interplay between light absorption and mixing (Stomp et al. 2007).

Role of T_{opt} and K_{sat}

For the example ensemble member in Fig. 4a, the assigned values of K_{sat} and T_{opt} were compared for the successful versus unsuccessful phytoplankton types (Fig. 8a,b). With 1000 phytoplankton types initialised, the assigned values of T_{opt} and K_{sat} clearly covered parameter space, although only a minority persisted with a biomass greater than 10^{-5} $\mu\text{M P}$.

For the nutrient sensitivity, phytoplankton types with low values of K_{sat} out-competed those with higher K_{sat} values (Fig. 8a,b), but this selection did not lead to vertical gradients in community structure (see Appendix 1: Test 2 for further evidence of this point). This successful competition can be explained by the open-ended Michaelis-Menten function for the nutrient-growth response, whereby, for any given nutrient concentration, a phytoplankton type with lower K_{sat} value yields a higher γ_j^N and therefore $P_{m,j}^C$, than one with a higher K_{sat} value. In this configuration, when K_{sat} was assigned randomly for the given ranges, there was no trade-off for a lower K_{sat} . This is a simplification of the complex traits and trade-offs that govern nutrient uptake, for example, causing the maximum uptake rate to co-vary with K_{sat} (Litchman et al. 2007). The selection for K_{sat} may be less important in nutrient replete regimes (Dutkiewicz et al. 2009).

For the temperature sensitivity, phytoplankton types had a competitive advantage at the depth where the *in situ* temperature was similar to their assigned value of T_{opt} (Fig. 8c,d). Since the temperature-growth function has upper and lower limits (Eq. 10), it follows that a phytoplankton type has a competitive advantage within a narrow range of *in situ* temperatures. In contrast to K_{sat} , temperature dependence was therefore important for vertical gradients in community structure, and selection based on temperature did not reduce the number of viable phytoplankton types (see Appendix 1: Test 3 for further evidence). Again, there was no associated trade-off for the temperature dependence in the model.

The stochastic framework employed in the model (Fig. 3) results in both K_{sat} and T_{opt} values for each successful phytoplankton type effectively being 'opti-

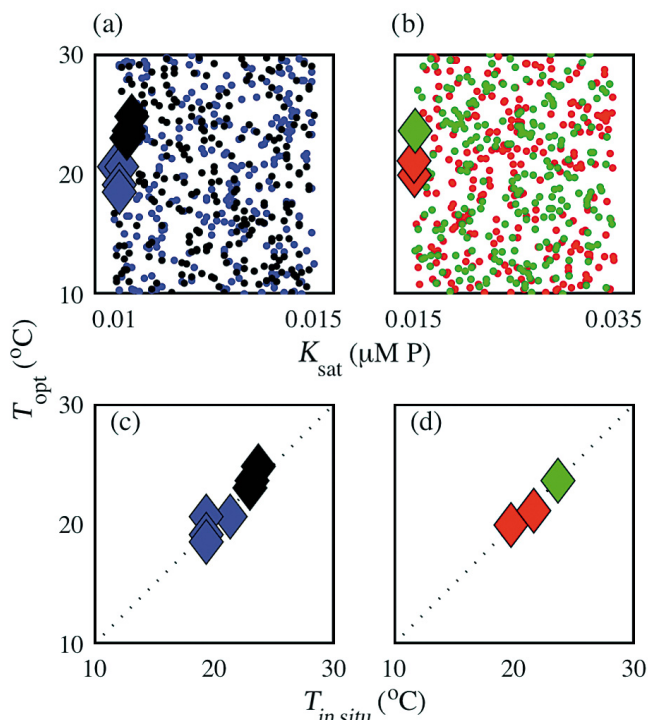


Fig. 8. Initialised parameter values for the example ensemble member shown in Fig. 4a. Values of the optimum temperature for growth, T_{opt} ($^{\circ}\text{C}$), against the nutrient half-saturation constant, K_{sat} ($\mu\text{M P}$), for all initialised phytoplankton types (dots) and successful phytoplankton types (diamonds), for (a) phytoplankton types with high-light *Prochlorococcus* (HLPro) absorption spectra (black) and low-light *Prochlorococcus* (LLPro) absorption spectra (blue), and (b) phytoplankton types with *Synechococcus* (Syn) absorption spectra (green) and eukaryote (Euk) absorption spectra (red). Values of T_{opt} against the temperature at the depth of the biomass maxima (at Month 10) for successful phytoplankton types with (c) HLPro absorption spectra (black) and LLPro absorption spectra (blue), and (d) Syn absorption spectra (green) and Euk absorption spectra (red). In (c) and (d), only the successful phytoplankton types are included; the 1:1 line is also shown. Successful phytoplankton types are those with biomass above 10^{-5} $\mu\text{M P}$ at Month 10, and subsequently those types visible in Fig. 4a

mised' for the environmental conditions. The optimisation of traits is in accord with the concept of evolutionary selection that leads to phytoplankton having multiple characteristics that suit them to a given environment. For example, high-light and low-light *Prochlorococcus* ecotypes have corresponding high and low T_{opt} , respectively (Zinser et al. 2007). The co-optimal adaptation of multiple traits between *Prochlorococcus* ecotypes also extends to their differential nitrogen sources (Moore et al. 2002) and underpins their biogeography (Johnson et al. 2006, Zinser et al. 2007). However, the combination of temperature and light dependence clearly involves a complicated interplay between traits and trade-offs (Zinser et al. 2007).

The simplified mixing regime in the model may have led to an overemphasised temperature gradient (Fig. 5a,b), and subsequently temperature-driven gradients in community structure above the DCM (Appendix 1: Fig. A1d). However, the selection for temperature occurs within, rather than between, spectral classes such that it does not influence our assessment of the importance of chromatic adaptation.

DISCUSSION

A stochastic, 'self-organising' model of marine phytoplankton was employed to investigate the role of chromatic adaptation in determining the vertical organisation of the phytoplankton communities in the oligotrophic oceans. We have implemented parameterisations of photoacclimation along with wavelength-dependent light absorption and radiative transfer in the model. One thousand phytoplankton types were each initialised with a unique set of physiological characteristics, including spectral light absorption properties, and the phytoplankton community was allowed to self-assemble through *in silico* 'survival of the fittest'.

The model was applied for a vertical profile in the South Atlantic Gyre, representative of the oligotrophic environment covering much of the ocean's mid-latitudes. The emergent profiles of phytoplankton biomass, chl *a* and vertical gradients in community structure of the phytoplankton were qualitatively consistent with observations from the Atlantic Meridional Transect, albeit with some contrasts in absolute values. Following a number of model thought experiments, the skill of the model in reproducing the community structure was strongly dependent on chromatic adaptation; the model's self-assembled phytoplankton community reflects a selective pressure from the photophysiology and pigments. Our demonstration of the importance of chromatic adaptation in an oceanic simulation is consistent with observational (e.g. Bidigare et al. 1990a, Ting et al. 2002, Lutz et al. 2003) and idealised model

studies (Stomp et al. 2004, Sathyendranath & Platt 2007).

In the model, organisation of the phytoplankton community was strongly affected by the inorganic nitrogen source, which segregated the water column into 2 broad groups: phytoplankton types that used nitrate (*Synechococcus* and eukaryotes) and those that did not (*Prochlorococcus*, or a subset thereof). The competition for spectral irradiance had a secondary influence on the coexistence between these 2 groups, most notably that phytoplankton types with absorption properties of the low-light *Prochlorococcus* had an advantage over those with absorption properties of the picoeukaryote at the DCM. Whether *Prochlorococcus* or eukaryotes dominate at the base of the euphotic zone thus depends on the co-availability of light and nutrients. Within the 2 broad groups controlled by the inorganic nitrogen source, pigments and photophysiology played a dominant role in structuring the community. Their spectral light requirements restricted *Synechococcus* to a surface water habitat due to competitive exclusion by eukaryotes at depth. In the surface, however, these 2 phytoplankters could coexist depending on their other traits. The spectral light requirements of the high- and low-light *Prochlorococcus* types did not lead to a vertical separation. Instead, realistic habitat organisation was only achieved when photoinhibition was imposed as a trade-off to the highly efficient light absorption of the low-light types. This role of photoinhibition for the absence of low-light *Prochlorococcus* ecotypes near the surface is consistent with culture and field studies (Moore & Chisholm 1999, Six et al. 2007, Zinser et al. 2007).

Multiple traits, here specifically the growth rate dependencies on light, nutrients and temperature, were co-optimal for the depths where phytoplankton types occurred in the water column. Thus, while optical properties play a role in the structuring of habitat, they represent just one of several factors that have co-evolved to be optimal in a particular environment and together shape the niches of different phytoplankton.

The model study made a number of simplifying assumptions in order to focus on the role of chromatic adaptation. *Prochlorococcus* ecotypes that could utilise nitrate (Casey et al. 2007), other size classes, or additional traits such as grazing defence, mixotrophy or mobility that potentially influence niche partitioning in the real ocean, were not explicitly included in the model. There were also simplifying assumptions about the chemical environment (such as a fixed uptake ratio for nutrients and no iron dependence) and the parameterisations for growth dependencies (such as the Eppley curve for temperature and Michaelis-Menten form for nutrient-dependent growth; Follows et al. 2007, Dutkiewicz et al. 2009). Although these simplifications may have influenced the resulting absolute

biomass values, they would not qualitatively alter the effect of spectral irradiance on species selection.

For this initial study, 4 phytoplankton types were chosen that had distinctly different light absorption spectra. The effects of photoacclimation and pigment packaging on the absorption spectra were not described, but were implicit in the culture measurements (Fig. 2). We subsequently assume that the 4 chosen types have absorption properties similar to the species within the groups they represent (i.e. *Synechococcus*, high-light and low-light *Prochlorococcus* and eukaryotes), and that spectral effects of acclimation are negligible compared to the difference in absorption properties between the groups. This assumption is reasonable, noting particularly that the picoeukaryote population in the oligotrophic regions also consists of flagellates that are of similar size and contain pigments that absorb light at similar wavelengths to our representative eukaryote, and that *Synechococcus* ecotypes with larger amounts of other phycobilins than are contained in our phycoerythrobilin-rich representative also occur in the oligotrophic ocean (Scanlan et al. 2009). While our simplified choices for the representative absorption spectra could have contributed to the mismatch in absolute biomass of the different types (Fig. 5c,d), as well as the community light absorption properties (Fig. 6b,c,e,f), between the model and the data, the model successfully reproduced the observed vertical gradients in community structure and revealed a clear role of chromatic adaptation that is consistent with observations. The importance of other phycobilins (phycourobilin and phycocyanobilin) within *Synechococcus*, or the range of pigment types within different eukaryotes could be explored in future studies.

Our results reveal co-optimality of multiple traits for a given niche, consistent with the evolutionary view. A key next step is exploring the interdependencies of traits and their physiological trade-offs (e.g. Litchman et al. 2007). For example, there is an interesting trade-off between light and nitrogen requirement in *Synechococcus*. Phycobilisomes are particularly rich in nitrogen (Raven 1984), creating a high nitrogen demand for the cells and, presumably, a preference for a nitrogen (and therefore nitrate)-rich environment. At the same time, the spectral dependence of absorption by these phycobilisomes favours a surface water habitat. The tension between these selective pressures may be important for the distribution of *Synechococcus* in the very oligotrophic central gyres, where they occur in near surface waters but do not dominate the phytoplankton biomass (Zubkov et al. 1998, 2000, Heywood et al. 2006). A complex ecosystem model, such as that used here, could provide a useful framework for future targeted studies into the interdependences of traits and trade-offs, and their role for community ecology.

In summary, we have demonstrated the importance of chromatic adaptation for shaping phytoplankton communities in the South Atlantic Gyre. The phytoplankton growth dependencies on light, nutrients and temperature were co-optimal, supporting the view that multiple traits have co-evolved to define an organism's niche. Although we have focussed on an oligotrophic environment, the processes and interactions explored here underpin phytoplankton selection and thus have a wider relevance to the global ocean.

Acknowledgements. We thank D. Suggett and L. Moore for providing culture data; J. Heywood and M. Zubkov for analytical flow cytometry measurements; L. Hay and G. Moore for spectral optical profiler data; the wider Atlantic Meridional Transect (AMT) community for providing ancillary data; and the officers and crew of RRS 'Discovery' during AMT-15. We also thank W. Gregg for valuable discussion on the optical framework and 5 anonymous referees for their insightful comments. This work was jointly funded through the UK Natural Environment Research Council (NERC) (grant NE/F002408/1), NASA (grant NNX09AE44G) and the Gordon and Betty Moore Foundation. The study was also supported by NERC through the AMT consortium (NER/O/S/2001/00680) and is contribution number 186 of the AMT programme. Participation of A.E.H. in AMT-15 was funded by a NERC PhD studentship.

LITERATURE CITED

- Babin M, Morel A, Claustre H, Bricaud A, Kolber Z, Falkowski PG (1996) Nitrogen- and irradiance-dependent variations of the maximum quantum yield of carbon fixation in eutrophic, mesotrophic and oligotrophic marine systems. *Deep-Sea Res I* 43:1241–1272
- Barlow RG, Aiken J, Holligan PM, Cummings DG, Maritorena S, Hooker S (2002) Phytoplankton pigment and absorption characteristics along meridional transects in the Atlantic Ocean. *Deep-Sea Res II* 47:637–660
- Bidigare RR, Marra J, Dickey TD, Iturriaga R, Baker KS, Smith RC, Pak H (1990a) Evidence for phytoplankton succession and chromatic adaptation in the Sargasso Sea during spring 1985. *Mar Ecol Prog Ser* 60:113–122
- Bidigare RR, Ondrusek ME, Morrow JH, Kiefer DA (1990b) In-vivo absorption properties of algal pigments. *Proc SPIE* 1302:290
- Bragg JG, Dutkiewicz S, Jahn O, Follows MJ, Chisholm SW (2010) Modeling selective pressures on picocyanobacterial nitrogen use in the global ocean. *PLoS ONE* 5:e9569, doi:10.1371/journal.pone.0009569
- Bricaud A, Stramski D (1990) Spectral absorption coefficients of living phytoplankton and nonalgal biogenous matter: a comparison between the Peru upwelling area and the Sargasso Sea. *Limnol Oceanogr* 35:562–582
- Casey J, Lomas MW, Mandecki J, Walker DE (2007) *Prochlorococcus* contributes to new production in the Sargasso Sea deep chlorophyll maximum. *Geophys Res Lett* 34:L10604, doi:10.1029/2006GL028725
- Chisholm SW (1992) Phytoplankton size. In: Falkowski PG, Woodhead AD (eds) Primary productivity and biogeochemical cycles in the sea. Plenum Press, New York, NY, p 213–237
- Conkright ME, Garcia HE, O'Brian TD, Locarnini RA, Boyer

- TP, Stephens C, Antonov JI (2002) World ocean atlas 2001, Vol 4. Nutrients. In: Levitus S (ed) NOAA Atlas NESDIS 52. US Government Printing Office, Washington, DC
- Dutkiewicz S, Follows MJ, Parekh P (2005) Interactions of the iron and phosphorus cycles: a three-dimensional model study. *Glob Biogeochem Cycles* 19:GB1021, doi:10.1029/2004GB002342
- Dutkiewicz S, Follows MJ, Bragg J (2009) Modeling the coupling of ocean ecology and biogeochemistry. *Glob Biogeochem Cycles* 23:GB4017, doi:10.1029/2008GB003405
- Eppley RW (1972) Temperature and phytoplankton growth in the sea. *Fish Bull* 70:1063–1085
- Follows MJ, Dutkiewicz S, Grant S, Chisholm SW (2007) Emergent biogeography of microbial communities in a model ocean. *Science* 315:1843–1846
- Geider RJ, MacIntyre HL, Kana TM (1997) Dynamic model of phytoplankton growth and acclimation: responses of the balanced growth rate and the chlorophyll *a*:carbon ratio to light, nutrient-limitation and temperature. *Mar Ecol Prog Ser* 148:187–200
- Gregg WW, Casey NW (2007) Modeling coccolithophores in the global oceans. *Deep-Sea Res II* 54:447–477
- Heywood JL, Zubkov MV, Tarran GA, Fuchs BM, Holligan PM (2006) Prokaryoplankton standing stocks in oligotrophic gyre and equatorial provinces of the Atlantic Ocean: evaluation of inter-annual variability. *Deep-Sea Res II* 53:1530–1547
- Hickman AE, Holligan PM, Moore CM, Sharples J, Krivtsov V, Palmer MR (2009) Distribution and chromatic adaptation of phytoplankton within a shelf sea thermocline. *Limnol Oceanogr* 54:525–536
- Jeffrey SW, Mantoura REC, Wright SW (1997) Phytoplankton pigments in oceanography: guidelines to modern methods. UNESCO, Paris
- Johnson ZI, Zinser ER, Coe A, McNulty NP, Woodward EMS, Chisholm SW (2006) Niche partitioning among *Prochlorococcus* phenotypes along ocean-scale environmental gradients. *Science* 311:1737–1740
- Kettle H, Merchant CJ (2008) Modeling ocean primary production: sensitivity to spectral resolution of attenuation and absorption of light. *Prog Oceanogr* 78:135–146
- Kirk JTO (1994) Light and photosynthesis in aquatic ecosystems. Cambridge University Press, Cambridge
- Kitidis V, Stubbins AP, Uher G, Upstill Goddard RC, Law CS, Woodward EMS (2006) Variability of chromophoric organic matter in surface waters of the Atlantic Ocean. *Deep-Sea Res II* 53:1666–1684
- Kywalyanga MN, Platt T, Sathyendranath S, Lutz VA, Stuart V (1998) Seasonal variations in physiological parameters of phytoplankton across the North Atlantic. *J Plankton Res* 20:17–42
- Ledwell JR, Watson AJ, Law CS (1993) Evidence for slow mixing across the pycnocline from an open-ocean tracer-release experiment. *Nature* 364:701–703
- Litchman E, Klausmeier CA, Schofield OM, Falkowski PG (2007) The role of functional traits and trade-offs in structuring phytoplankton communities: scaling from cellular to ecosystem level. *Ecol Lett* 10:1170–1181
- Lutz VA, Sathyendranath S, Head EJH, Li WKW (2003) Variability in pigment composition and optical characteristics of phytoplankton in the Labrador Sea and the Central North Atlantic. *Mar Ecol Prog Ser* 260:1–18
- Moore LR, Chisholm SW (1999) Photophysiology of the marine cyanobacterium *Prochlorococcus*: ecotypic differences among cultured isolates. *Limnol Oceanogr* 43:628–638
- Moore LR, Goericke R, Chisholm S (1995) Comparative physiology of *Synechococcus* and *Prochlorococcus*: influence of light and temperature on growth, pigments, fluorescence and absorptive properties. *Mar Ecol Prog Ser* 116:259–275
- Moore LR, Rocap G, Chisholm SW (1998) Physiology and molecular phylogeny of coexisting *Prochlorococcus* phenotypes. *Nature* 393:464–466
- Moore LR, Post AF, Rocap G, Chisholm SW (2002) Utilization of different nitrogen sources by the marine cyanobacteria *Prochlorococcus* and *Synechococcus*. *Limnol Oceanogr* 47:989–996
- Partensky F, Blanchot J, Lantoin F, Neveux J, Marie D (1996) Vertical structure of picophytoplankton at different trophic sites of the tropical northeastern Atlantic Ocean. *Deep-Sea Res I* 43:1191–1213
- Pope RM, Fry ES (1997) Absorption spectrum (380–700 nm) of pure water. II. Integrating cavity measurements. *Appl Opt* 36:8710–8723
- Rabouille S, Edwards CA, Zehr JP (2007) Modelling the vertical distribution of *Prochlorococcus* and *Synechococcus* in the North Pacific Subtropical Ocean. *Environ Microbiol* 9:2588–2602
- Raven JA (1984) A cost-benefit analysis of photon absorption by photosynthetic unicells. *New Phytol* 98:593–625
- Rocap G, Larimer FW, Lamerdin JW, Malfatti S and others (2003) Genome divergence in two *Prochlorococcus* phenotypes reflects oceanic niche differentiation. *Nature* 424:1042–1047
- Sathyendranath S, Platt T (2007) Spectral effects in bio-optical control on the ocean system. *Oceanologia* 49:5–39
- Scanlan DJ, Ostrowski M, Mazard S, Dufresne A and others (2009) Ecological genomics of marine picocyanobacteria. *Microbiol Mol Biol Rev* 73:249–299
- Six C, Finkel ZV, Irwin AJ, Campbell DA (2007) Light variability illuminates niche-partitioning among marine picocyanobacteria. *PLoS ONE* 2:e1341, doi:10.1371/journal.pone.0001341
- Stephens C, Antonov JI, Boyer TP, Conkright ME, Locarnini RA, O'Brian TDO, Garcia HE (2002) World ocean atlas 2001, Vol 1. Temperature. In: Levitus S (ed) NOAA Atlas NESDIS 49. US Government Printing Office, Washington, DC
- Stomp M, Huisman J, de Jongh F, Veraart AJ and others (2004) Adaptive divergence in pigment composition promotes phytoplankton biodiversity. *Nature* 432:104–107
- Stomp M, Huisman J, Vörös L, Pick FR, Laamanen M, Haverkamp T, Stal LJ (2007) Colourful coexistence of red and green picocyanobacteria in lakes and seas. *Ecol Lett* 10:290–298
- Suggett DJ, MacIntyre HL, Geider RJ (2004) Evaluation of biophysical and optical determinations of light absorption by photosystem II in phytoplankton. *Limnol Oceanogr Methods* 2:316–332
- Suggett DJ, Moore CM, Hickman AE, Geider RJ (2009) Interpretation of fast repetition rate (FRR) fluorescence: signatures of phytoplankton community structure versus physiological state. *Mar Ecol Prog Ser* 376:1–19
- Ting CS, Rocap G, King J, Chisholm SW (2002) Cyanobacterial photosynthesis in the oceans: the origins and significance of divergent light harvesting strategies. *Trends Microbiol* 10:134–142
- Tomo T, Akimoto S, Ito H, Tsuchiya T, Fukuya M, Tanaka A, Mimuro M (2009) Replacement of chlorophyll with divinyl chlorophyll in the antenna and reaction centre complexes of the cyanobacterium *Synechocystis* sp. PCC 6803: characterisation of spectral and photochemical properties. *Biochim Biophys Acta* 1787:191–200

- Williams RG, Follows MJ (1998) The Ekman transfer of nutrients and maintenance of new production over the North Atlantic. *Deep-Sea Res I* 45:461–489
- Wood AM (1985) Adaptation of photosynthetic apparatus of marine ultraphytoplankton to natural light fields. *Nature* 316:253–255
- Zinser ER, Johnson ZI, Coe A, Karaca E, Veneziano D, Chisholm SW (2007) Influence of light and temperature on *Prochlorococcus* phenotype distributions in the Atlantic

- Ocean. *Limnol Oceanogr* 52:2205–2220
- Zubkov MV, Sleigh MA, Tarran GA, Burkill PH, Leakey RJG (1998) Picoplanktonic community structure on an Atlantic transect from 50° N to 50° S. *Deep-Sea Res I* 45: 1339–1355
- Zubkov MV, Sleigh MA, Burkill PH, Leakey RJG (2000) Picoplankton community structure on the Atlantic Meridional Transect: a comparison between seasons. *Prog Oceanogr* 45:369–386

Appendix 1. Thought experiments

To further examine the importance of light absorption spectra, temperature and nutrient requirements, we performed an additional suite of thought experiments. One ensemble member for the full model scenario (Figs. 4a & A1a) following the framework outlined in Fig. 3, was re-run a series of times (Fig. A1b–d), each time with either the chl *a*-normalised light absorption characteristics, $a_j^{chl}(\lambda)$ paired with $a_{ps,j}^{chl}(\lambda)$, the optimum temperature for growth (T_{opt}) and the half-saturation constant (K_{sat}) fixed to the same value for all phytoplankton types, thereby removing them sequentially from the selection process. Since the same initialisation was used for each experiment, the assigned characteristics for each phytoplankton type were identical to those in the example ensemble (Fig. A1a) unless they were artificially chosen to be the same for all phytoplankton types. These experiments therefore reveal how the different growth-dependencies influence the community structure, which in combination result in the phytoplankton distributions observed in the full model outcome.

Test 1. Same K_{sat} and T_{opt} for all phytoplankton types, realistic absorption spectra assigned (Fig. A1b)

In the first experiment, T_{opt} and K_{sat} were the same for all phytoplankton types ($K_{sat} = 0.015 \mu\text{M P}$ for all types that used nitrate and $0.01 \mu\text{M P}$ for all types that did not; $T_{opt} = 22^\circ\text{C}$), while light absorption properties representative of either *Synechococcus* (Syn), eukaryotes (Euk), high-light *Prochlorococcus* (HLPro) or low-light *Prochlorococcus* (LLPro) were assigned as normal (Fig 3). The phytoplankton types thus differed according to their nutrient sources and light absorption properties (and photoinhibition for phytoplankton types with LLPro absorption spectra).

Since there was no stochastic assignment for T_{opt} and K_{sat} , there were only 6 possible combinations of characteristics, and many of the 1000 initialised phytoplankton types were identical (see Fig. 3), such that this result is trivially identical for any initialisation. The difference in the biomass of types with Syn absorption spectra, e_{syn} , compared to those with Euk spectra, e_{euk} , was subsequently solely due to their dif-

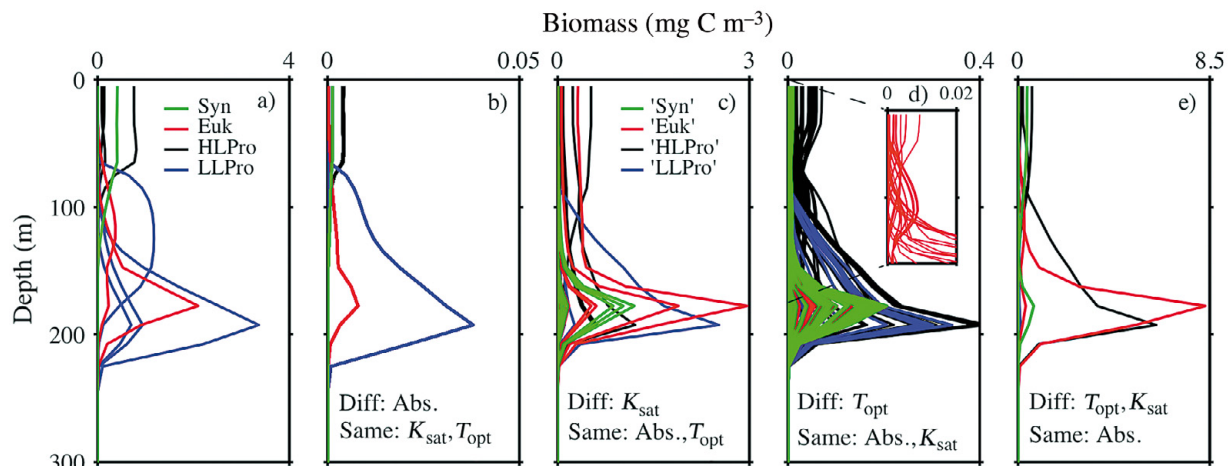


Fig. A1. (a) Vertical profiles of carbon biomass for all phytoplankton types for one ensemble member. Phytoplankton types are identified according to their light absorption properties. (b) to (e) Results of thought experiments whereby the example ensemble member (in a) was re-run with chosen characteristics assigned to be the same for all phytoplankton types; see Appendix 1 text for details. The inset in (d) is an enlarged region 0 to 175 m for a subset of 20 phytoplankton types (that, arbitrarily, have eukaryote [Euk] absorption spectra), highlighting the vertical gradients caused by different optimum temperature (T_{opt}) values. Where identical spectral light absorption properties were assigned for all phytoplankton types, the light absorption spectrum was the mean (at each wavelength) of the high-light *Prochlorococcus* (HLPro), low-light *Prochlorococcus* (LLPro), Euk and *Synechococcus* (Syn) spectra shown in Fig. 2. Mean spectra were obtained for both the light absorption by all pigments, and the light absorption by photosynthetic pigments. Subsequently, as indicated by quotation marks, coloured lines in (c) to (e) represent the absorption spectra that would have been assigned for each of the phytoplankton types in the full model run, and thus allow direct comparison with (a). K_{sat} : half-saturation constant; Diff.: characteristics that differed between types (values as in the full model run); Abs.: absorption spectra

Appendix 1 (continued)

ferences in light absorption properties. This result shows that the light absorption properties allow coexistence of e_{syn} and e_{euk} towards the surface, resulting from their utilisation of different components of the light spectrum (Stomp et al. 2004, 2007). Further, it reveals an advantage for Syn compared to Euk spectra towards the surface, given the higher biomass for e_{syn} (Fig. A1b). The dominant effects of spectral absorption properties and photoinhibition discussed in the main text also describe the vertical separation of phytoplankton types with HLPro and LLPro absorption properties in this experiment.

This experiment revealed similar vertical gradients in community composition as observed for the ensemble mean of the full model (Fig. 5d).

Test 2. Same T_{opt} and absorption spectra for all types, K_{sat} assigned stochastically (Fig. A1c)

In the second thought experiment, all phytoplankton types were provided with the same (mean) light absorption spectra and a constant value for T_{opt} ($T_{\text{opt}} = 22^{\circ}\text{C}$), while K_{sat} was assigned stochastically. The line colours in Fig. A1c represent the absorption spectrum and were assigned for directly corresponding phytoplankton types in the full model, even though the light absorption properties are now the same for all types. This enables a comparison to the distributions in the full model outcome (Fig. A1c). Accepting that photoinhibition and the nitrogen resource requirements caused some vertical structure within the non-nitrate-using phytoplankton types, there were no apparent vertical shifts in community structure caused by the contrasting values of K_{sat} . The selection for low K_{sat} values (Fig. 8a,b) strongly influenced which phytoplankton types were successful and significantly reduced the number of viable types. However, the successful types were consistently dominant at all depths. Thus, in the full model, the selection for K_{sat} values reduced the number of potentially successful phytoplankton types (and all successful types had low K_{sat} values) but did not significantly influence the vertical gradients in community structure.

Test 3. Same K_{sat} and absorption spectra for all types, T_{opt} assigned stochastically (Fig. A1d)

In the third thought experiment, all phytoplankton types had the same (mean) light absorption spectra and the same K_{sat} value ($K_{\text{sat}} = 0.015 \mu\text{M P}$ for all phytoplankton types that used nitrate and $0.01 \mu\text{M P}$ for those that did not), while T_{opt} was assigned stochastically. Variations in the value of T_{opt}

and corresponding competition on the temperature gradient (Fig. 8c,d), caused fine-scale vertical gradients in the community structure through the water column (inset in Fig. A1d). This selection on the temperature gradient was responsible for the success of numerous different phytoplankton types within the light resource groupings, for example, the multiple phytoplankton types with LLPro absorption spectra (i.e. blue lines) in the full ensemble member (Fig. A1a). Selection due to the temperature dependence did not reduce the number of successful phytoplankton types.

The vertical gradients in community structure observed in the full model outcome were thus dependent on the temperature dependence; phytoplankton types that were successful towards the surface had high values of T_{opt} , whilst those successful at depth had lower values of T_{opt} .

Test 4. Same absorption spectra for all types, T_{opt} and K_{sat} assigned stochastically (Fig. A1e)

In a final thought experiment, all phytoplankton types had the same (mean) light absorption spectra, whilst T_{opt} and K_{sat} were assigned stochastically. This experiment thus represents an ensemble member that contributed to the mean shown in Fig. 7b. Although not identical, there were similarities between this experiment (Fig. A1e) and the ensemble outcome from the full model (Fig. A1a). For example, in the ensemble from the full model (Fig. A1a), a phytoplankton type with Syn absorption spectra dominated at the surface, whilst in the experiment (Fig. A1e), this also occurred, albeit by chance due to the assigned T_{opt} and K_{sat} values, rather than spectral light absorption properties. Similarly, K_{sat} and T_{opt} were optimal for growth at the DCM for the phytoplankton type also assigned Euk absorption spectra in the example ensemble (Fig. A1a,e). It follows that in the full example ensemble member (Fig. A1a), the successful phytoplankton types with Euk and Syn light absorption properties had dependencies on temperature, nutrients and light that were co-optimal. Successful phytoplankton types in the full model therefore also, on average, had a co-optimal combination of traits.

In summary, this series of thought experiments reveals how the spectral light properties, K_{sat} and T_{opt} act on phytoplankton selection. Crucially, the model preferentially selected for phytoplankton with co-optimal traits. Thus, the successful phytoplankton types in the ensemble mean (Fig. 5) had, in addition to their dependence on spectral irradiance, low half saturation constants for nutrient uptake and temperature optima suitable for the depth at which they occurred in the water column.